

## EXPLORING RESEARCHES ON THE SPACE-TIME EFFECTS OF HYPERBOLIC FIELDS

D. G. PAVLOV<sup>1</sup>, S. S. KOKAREV<sup>1,2</sup>, M. S. PANCHELYUGA<sup>1,3</sup>  
and V. A. PANCHELYUGA<sup>1,3</sup>

Communicated to the conference:

*Finsler Extensions of Relativity Theory, Braşov, Romania, Aug. 20 - Sept. 4, 2011*

### Abstract

The paper presents preliminary results of experiments designed to search for hyperbolic or H-fields, which, according to the theoretical representations developed in [1–15], should lead to a local modification of the flow of time. As a generator of the H-field, it is used a process of mechanical strike and as a detector, a highly stable quartz generator. The result of the influence of the H-field on the quartz generator has to be a modification of its oscillation parameters. In the experiment, it is discovered a shift of the power spectrum of oscillation of the quartz generator in the moment of the strike, in comparison with the spectrum in control, obtained under the same conditions, but without the strike. The theoretical estimates given in the paper for the acoustic, electromagnetic and gravitational wave mechanisms of influence of the strike on the oscillations of the quartz generator prove that these mechanisms cannot produce any experimentally observable spectrum shift, either from the qualitative or from the quantitative point of view.

*Key words:* Finsler geometry, Berwald-Moor metric, hyperbolic fields, quartz generator.

### 1 Introduction. Ideas underlying the experiments

In the papers [1–15], it was discussed the idea of the description of the geometry of the real physical space-time in terms of various generalizations of the standard Minkowski metric:

$$dS^2 = c^2 dt^2 - dx^2 - dy^2 - dz^2, \quad (1)$$

---

<sup>1</sup>Research Institute of Hypercomplex Systems in Geometry and Physics, Fryazino, Russia, e-mail: geom2004@mail.ru, logos-center@mail.ru, panvic333@yahoo.com

<sup>2</sup>Regional Scientific-Educational Center "Logos", Yaroslavl, Russia

<sup>3</sup>Institute of Theoretical and Experimental Biophysics of the Russian Academy of Sciences, Pushchino, Russia

by metrics of Finsler type. One of these generalizations is the 4-dimensional Berwald-Moor metric:

$$dS^4 = C^4 (dt^4 + dt_1^4 + dt_2^4 + dt_3^4 - 2(dt^2 dt_1^2 + \dots + dt_2^2 dt_3^2) + 8dt dt_1 dt_2 dt_3), \quad (2)$$

which is interesting by the fact that it has a tight relation with commutative-associative 4-numbers, in a total analogy with the relation between Euclidean geometry and complex numbers. Moreover, the problem of the inclusion of the metric (1) into (2) is nontrivially solved by means of the so-called tangent construction [16]. The attempt of description of physical reality by means of the interval (2) instead of (1) opens, besides approaches for the discovery of essentially new regularities and effects, new perspectives of research and explanations of already known phenomena. In any case, the decisive (though not unique) criterion of selection of fundamental hypotheses is experiment. Details, preliminary results and an analysis of one of the undertaken and performed experiments, which motivate polynumber field theories [16] and the underlying Finsler geometry with interval (2), are presented in this paper. The considerations providing the motivation of the proposed experiment are related to the general idea of the relation of space-time symmetries with physical fields and field equations. It is well known that sourceless Maxwell's equations are invariant under the action of the 15-parameter group of conformal symmetries of the interval (1). Besides, from a historical point of view, Maxwell's equations, whose structure contains relativistic properties of space-time, appeared much earlier than the principles of special relativity theory. On the other side, as shown in the papers [12, 13], the interval (2) admits an infinite-dimensional group of conformal symmetries. This group is described by holomorphic functions of 4-numbers and has an analogous structure to the one of the group of conformal symmetries of the Euclidean plane, which consists of holomorphic functions of a complex variable. This way, one can expect that in the space-time with interval (2), there should exist some fields associated with the infinite-dimensional group of symmetries of this interval, obeying field equations which are invariant with respect to this group. The theory of these fields (it was proposed to call them hyperbolic or H-fields) was studied in the papers [15–18]. In particular, in [18], based on the 2-dimensional version of the interval (2), which describes nothing else than the 2-dimensional Minkowski space-time, it was developed an algebraic nonlinear unified theory of space, time and matter. This theory, as well as its generalization to higher dimensions, will be regarded as a general basic platform for a unified description of matter, gravity, electromagnetism and possibly, of other interactions, alternative to the generally accepted theories. The theory of hyperbolic fields is interesting and, in our opinion, it is a fruitful symbiosis of the ideas of complex potential theory, of Weyl, Kaluza-Klein and Mie's unified theories and also of several key concepts of special and general relativity.

One of the predictions of this theory is the effect of deformation of space-time scales in a domain without sources, in which there exists a hyperbolic field. In particular, an inhomogeneous field creates a difference in the measurements of two identical, spatially distant clocks. In a certain sense, the sought hyperbolic fields manifest themselves in the same way as fields of 4-velocities of world lines of particles in the pseudo-Euclidean space-time, with the only difference that the module of the pseudo-Euclidean 4-velocity

is always equal to 1, while in the Finslerian space-time, the module of the 4-velocity can take also values different from 1.

In order to register the effects of the local deformation of space-time scales, it is necessary to choose a relatively simple and convenient source of hyperbolic fields and a sensitive enough way of detecting them.

In our experiment, as a generator of hyperbolic fields, we took a device which produces the strike of a weight on an immobile anvil. In the process of hitting, there appear intense deformations and transformations of the kinetic energy of the weight into other types of energy on different channels. It is possible (the question on the sources of hyperbolic fields as a whole still remains open), that precisely such conditions contribute to the generation of hyperbolic fields whose intensity is sufficient to produce detectable effects. As detectors, we use highly accurate quartz generators, situated at various distances from the points where the strikes take place. The essence of the experiment consists in the comparison of several averaged characteristics of the work of a quartz generator during the strike and afterwards.

The experiment proposed by us has to be regarded as a preliminary, exploring one (as indicated in the title of this paper) and, to a great extent, qualitative. Nevertheless, in our opinion, the results of the experiment, which are exposed in detail in the second part of the article and their preliminary analysis, presented in the third part, are, as a whole, encouraging and represent the basis for the organizing and performing of further, more detailed, experimental research.

## 2 Experimental research of the manifestation of hyperbolic fields. Preliminary results

### 2.1 Generator of hyperbolic fields

As we have already mentioned, as a generator of H-fields, it is proposed to use a process of mechanical strike. With this aim, it was built a 12 m high tower, shown in Fig. 1. The tower is used for: lifting the weight at a given height, automatically releasing it and for directing its fall over a steel anvil. The weight is fixed in a special sliding device, which slides inside the tower and serves to direct it, performing the lifting of the weight and also direct its fall precisely to the center of the anvil. In the picture 2, one can see the weight, fixed in the sliding device, the anvil and the lower part of the tower, which directs the sliding device in which the weight is fixed.

The steel anvil lays on the concrete floor of a special well. The upper edge of the well serves as ground for the tower, which is held in a vertical position by means of a system of cables. In its upper part, the well is closed by a waterproof flooring, in which there is a hatch allowing the descent into the well. The tower, the weight, the well, the anvil, the weight lifting system, consisting of a windlass and a steel cable with a fixing system of the weight, producing its automatic release when a given height is reached, are shown in the left side of Fig. 3.

In the right side of Fig. 3, it is shown a covered measuring pit, having the same depth as the well. The pit is situated at a distance of 1.5 m. from the well. It serves as a location for measuring devices and also, it allows to significantly weaken the acoustic



Fig. 1: Photo of the tower used in the process of mechanical hitting.

radiation generated in the moment when the weight hits the anvil.

## 2.2 Quartz generators used

For the experiment, we chose highly stable double ovenized quartz generators GK-216-TS, produced by the company MORION. The generators have a low level of phase noise. They are vacuumed and electromagnetically shielded. Some parameters of the quartz generator, guaranteed by the manufacturer, are shown in Table 1.

As follows from the presented table, the instability of the frequency of the quartz generators used in the experiment, for a measuring time of 2-4 hours (used in the current experiment), does not exceed  $10^{-10} \dots 10^{-11}$ .

In Fig. 4), it is given an example of record of the output signal of the quartz generator. As one can see, the output signal is a pure sinus with no visible nonlinear distortions. The quality of such a signal also confirms its power spectrum – shown in Fig. 4 b) and represented as a unique sharp peak at the resonance frequency of the quartz generator. A more detailed research of the power spectrum (Fig. 5) also reveals the presence of a weak second harmonic at a frequency of 20 MHz, as well as some oscillation mode in the neighborhood of the frequency of 5 MHz.



Fig. 2: The guiding system, the weight and the anvil.

### 2.3 Registering system

The flowchart of the recording system is represented in Fig. 6. It consists of the above described quartz generator (QG), placed in a hermetic metallic body, the power supply of the quartz generator (PS), an ultrasonic sensor of the strike (US-sensor), a digital storage oscilloscope WaveJet 322A of the company LeCroy (DSO), allowing a high-speed (up to 1GS per channel) synchronous sampling of the output signals, with the possibility of further storage of the obtained results in the memory of a personal computer (PC). The built-in memory of the DSO ensures the registration of 500000 successive measurements per channel.

The registering system shown in Fig. 6 is designed for measurements of two types: control (the signal of the generator is recorded in the absence of any strike) and experiment (it is registered the part of the signal corresponding to the proximity of the moment of the strike). As an example of a control measurement, one can take the sinusoidal signal shown in Fig. 4 ).

The registering process of the measured signal takes place as follows. At the inputs of the DSO, are the output signals from the quartz generator (shown in dark blue on Fig. 7 and from the output of the US-sensor (drawn with red color in Fig. 7). The signals are continuously digitized and cyclically recorded in its built-in memory. In the moment when the weight first touches the anvil, it arrives the signal from the US-sensor, which launches the synchronizing system of the DSO in such a way that in the memory of the oscilloscope it is stored the part of the signal preceding the moment of first touches and it is also registered a part of the signal of the same duration, after this moment. This way, the resulting record contains the output signal from of the quartz generator before the strike and during it. Examples of recordings in the proximity of the strike moment are represented in Fig. 7. The signals shown in Fig. 7 were digitized with the frequency of 250 Hz, the length of the registration is of 500000 points, which all in all corresponds to

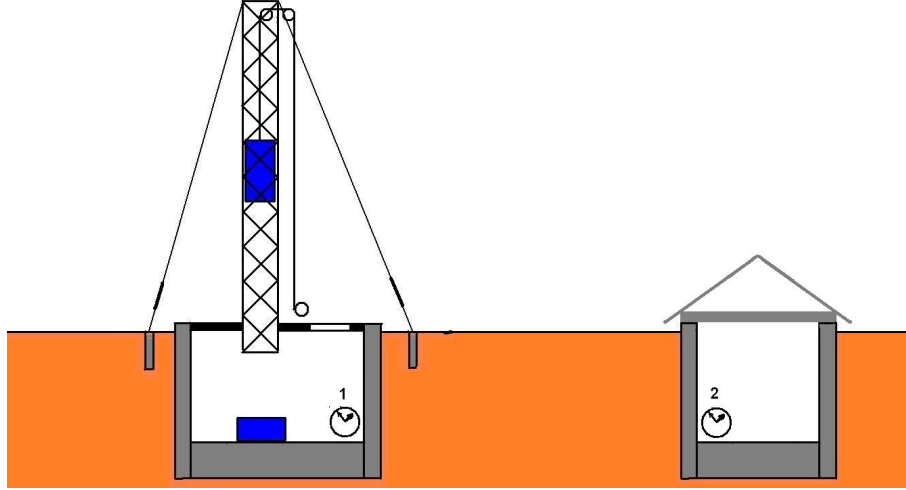


Fig. 3: Scheme of the tower and of the measuring pit.

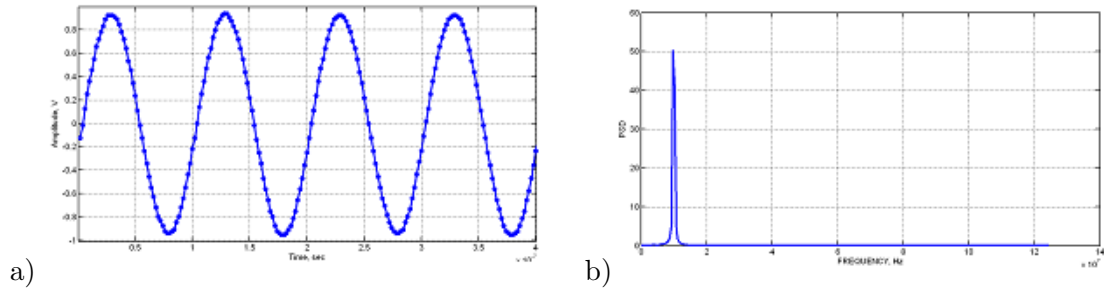


Fig. 4: Output signal of the generator, a), and its power spectrum, b).

a time interval of 2 msec. The set of researches we performed proved that this duration is optimal, on one side, in order to register the proximity of the moment of the strike and on the other — to receive a qualitative record of the signal of the generator (25 points for a period).

At the same time, as shown in Fig. 7, each strike of the weight on the anvil has its individual portrait, unrepeatable from a strike to another. Thus, the method for measuring and for data processing, presented in this paper, implies operating with parameters averaged over the set of measurements.

## 2.4 Measurement method

In order to exclude a possible influence of external factors on the final result, we used the measurement method with alternation. Its essence consists in the fact that after each measurement made in the moment when the weight hits the anvil, it is made a control measurement - the registration of the signal of the unperturbed (i.e., without the strike) quartz generator. This way, the experiment and the control alternate on the whole duration of the series of measurements. The average time during which it takes place the

Table 1: Parameters of the used quartz generators.

Nominal frequency	10 MHz
Output signal	sinus
Temperature instability in the temperature range $-10 \dots +60^{\circ}\text{C}$	$\pm 1 \times 10^{-10}$
Long term instability of the frequency, not more than	$\pm 5 \times 10^{-9}$ (1 year) $\pm 3 \times 10^{-8}$ (10 years)
Short term instability of the frequency (Allan deviation) per averaged time 1 sec.	$< 2 \times 10^{-12}$
Temperature range	$-55 \dots +80^{\circ}\text{C}$
Mechanical strike (crashworthiness)	100g/3 $\pm$ 1 mc
Resistance to sinusoidal vibrations (vibration resistance)	1-200 /5 g
Hermetic seal	The generator is hermetically sealed

registering of one pair experiment-control is of 5 minutes. Usually, the climate factors (humidity, pressure, temperature etc.), significant variations of the geophysical fields have a periodicity which exceeds this value. This is why for a series of measurements taking place, usually, for 2.5 — 4 hours, they have to be averaged, if we want to examine the difference between the averaged values of some parameter between experiment and control.

## 2.5 Processing of the experimental data. Difference spectrum.

The measurement method "with alternation" follows from the following ideas of processing experimental data. It is made a large enough quantity of successive experimental (in the moment of the strike) and control recordings of the signal of the quartz generator. As a result, we obtain two sets of time sequences. For each time sequence, one calculates the power spectrum. After this, using the individual (for each time sequence) power spectra, one calculates the average power spectra for each of the sets. As a result, we obtain the average power spectra for the series of measurements in the moment of the strike and for the control series. Subtracting them, we get the difference spectrum. In the case when the result of the subtraction is a nonzero difference spectrum, we can speak about the existence of a certain frequency shift between the control measurements and those performed in the moment of the strike, which in its turn has to testify about the existence of the sought interaction. In Section 3.1.3, it is examined the transformation of the shape of the difference spectrum as a function of different types of change of the average spectra.

We have performed two series of measurements, which differ by the distance from the

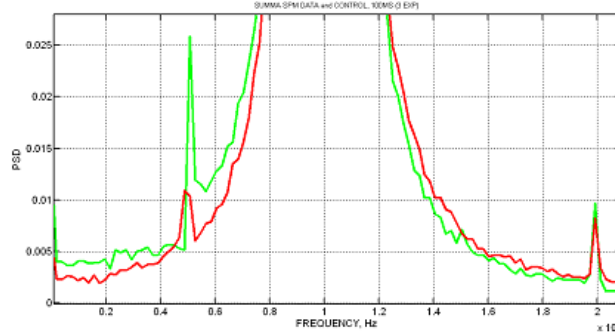


Fig. 5: Zoomed part of the plot of the power spectrum of the oscillation of two quartz generators in the neighborhood of the main harmonic.

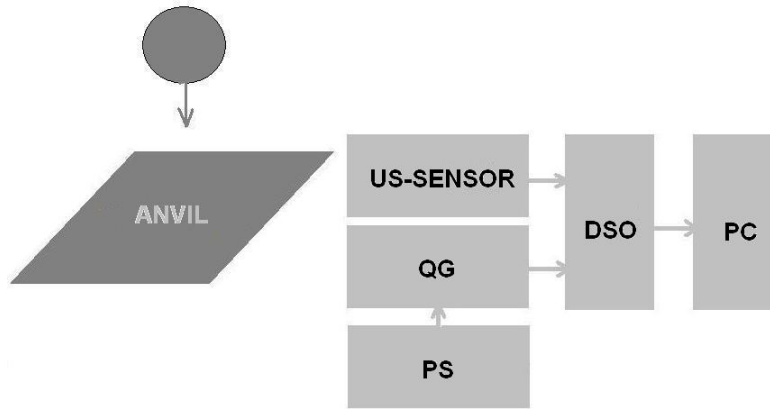


Fig. 6: Flowchart of the registering system.

center of the anvil to the quartz generator. The positions of the quartz generator we used are denoted on Fig. 3 by digits on a symbolic image of a clock. In the first position, the quartz generator was situated in the well at a distance of 0.5 meters from the center of the anvil and, in the second one — in the measuring pit, at a distance of 3.2 m from the center of the anvil.

In Fig. 8, we present the average power spectra for the measurements in the moment of the strike, Fig. 8 a), and the control ones, Fig. 8 b). As one can see, the obtained spectra are visually perfectly identical – which one might expect, taking into account that the measurements in both series were made with the same quartz generator, maximally protected from external influences. But the subtractions of the spectra shown in Fig. 8 show that between them there exist very small differences, which can be very well seen in Fig. 9. The result represented in Fig. 9, as shown in 3.1.3, allows us to speak about a frequency shift between the measurements during the experiment and the control ones, which can testify about the generating, in the moment of the strike, of H-fields.

The results for the series of measurements in the pit (position 2 on Fig. 3) are repre-

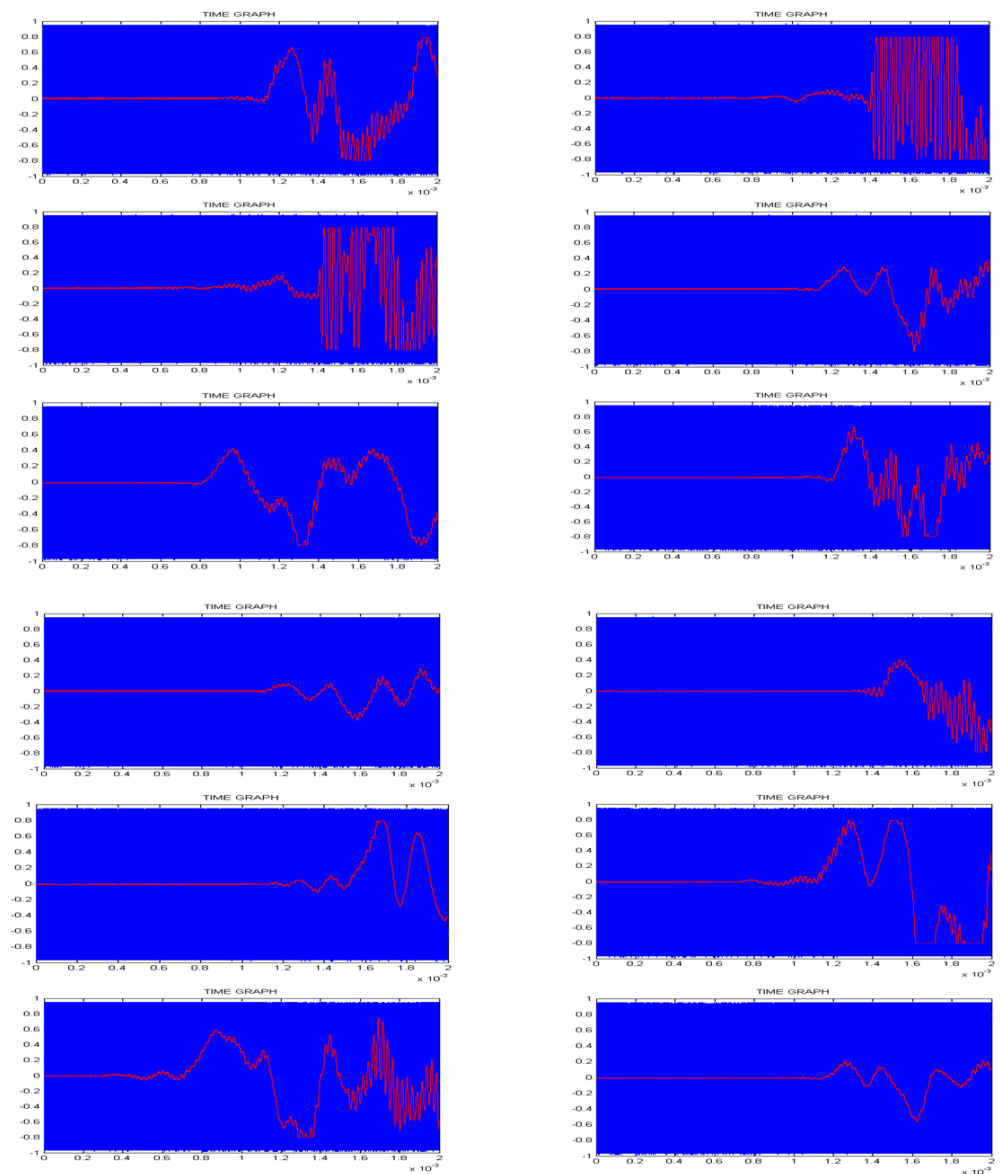


Fig. 7: Examples of registrations of the moment of the strike.

sented in Fig. 10 and Fig. 11. Here, just as for the measurements in the well, we obtained the average spectra for the experiment measurements, Fig. 10 a) and the control ones, Fig. 10 b), which, as in the previous case, do not reveal any visible difference. The differences become visible only for the differences of total spectra, shown in Fig. 11.

In Fig. 11 it can be seen an interesting feature: in comparison to Fig. 9, the oscillation mode in the domain of 5 MHz reduced its amplitude significantly less than in the case of a basic oscillation mode with a frequency of 10 MHz. This fact needs a special attention in further experiments.

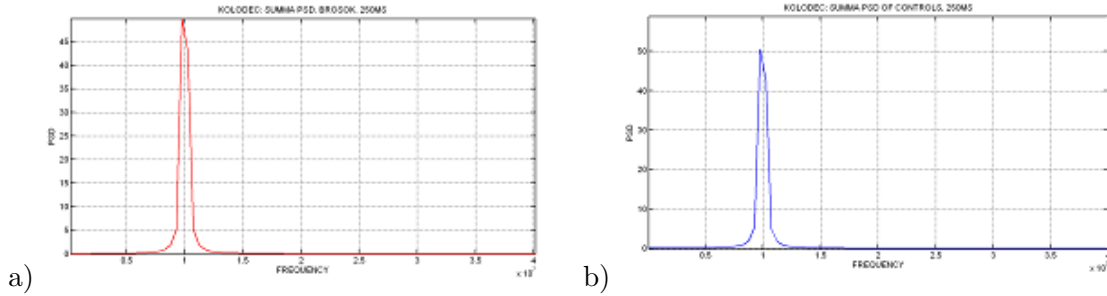


Fig. 8: Average power spectra for measurements in the well: a) measurement in the moment of the strike, b) control measurements.

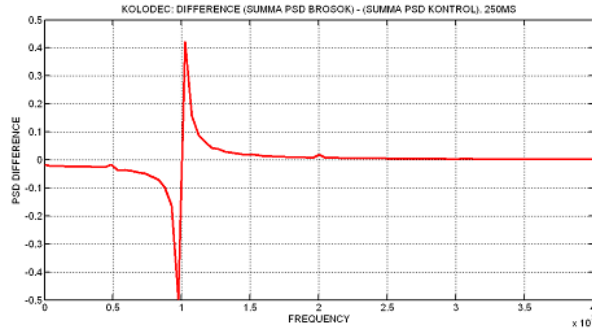


Fig. 9: Difference of total spectra (Fig. 8) for measurements in the well.

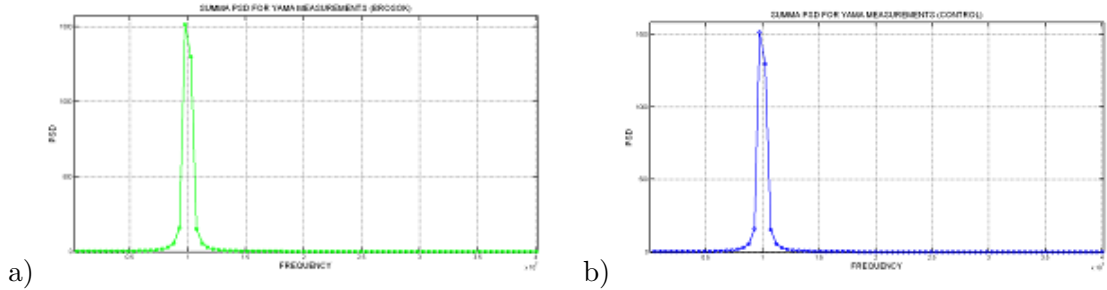


Fig. 10: Average power spectra for the measurements in the pit: a) measurements in the proximity of the moment of the strike, b) control measurements.

For the convenience of the comparison in Fig. 12, we have presented the differences of average spectra for the series of measurements in the well (KOLODEC) and in the pit (YAMA). It can be seen that for the case when the measurements are performed in the pit, the amplitude of the effect is much lower. From Fig. 9 and Fig. 11, we can roughly evaluate the value of the frequency shift. For the measurements in pit, the distance on the x-axis between the positive and the negative maxima is equal to 12 kHz, for the measurements in the well — 180 kHz. Consequently, for the measurements in the pit, the frequency shift

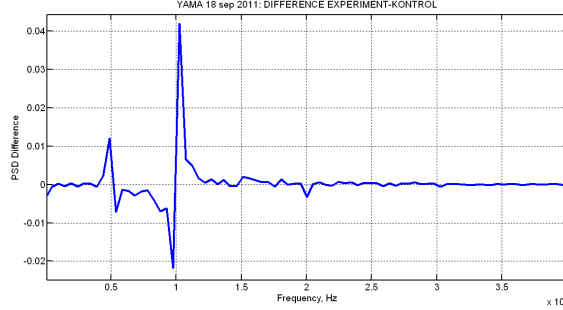


Fig. 11: Difference of average spectra (Fig. 10) for the measurements in the pit.

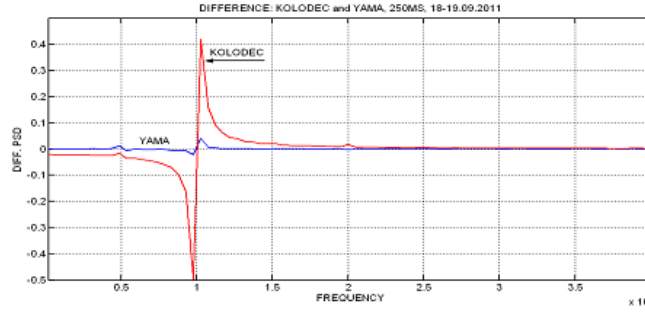


Fig. 12: Differences of the total spectra for the series of measurements in the well (red) and in the pit (dark blue).

can be of 1-2 kHz, for the measurements in the well, the effect value is approximately 36 kHz.

### 3 Theoretical estimates of the influence of acoustic, electromagnetic and wave-gravitational perturbation upon the power spectrum of the quartz generator.

#### 3.1 Simplified working model of the oscillations of the quartz generator

We will consider the quartz generator as an oscillating system which, in the absence of perturbations is characterized by a power spectrum of the form

$$G(I, \sigma, \omega_0, \omega) = |U_\omega|^2 = I e^{-(\omega - \omega_0)^2 / \sigma^2}, \quad (3)$$

where the parameters  $\omega_0$ ,  $\sigma$  and  $I$  have the meaning of resonance frequency of oscillations, width of the spectral curve and maximum of the spectrum accordingly. The quantity  $U_\omega$  is the Fourier transform  $U(t)$  of the output voltage of the generator. This quantity is related by the coefficient  $K$

$$U(t) = KV(t) \quad (4)$$

to the voltage  $V(t)$  on the electrodes of the quartz plate, which is included in a feedback circuit and acts on the resonance frequency by means of the piezoelectric effect.

### 3.1.1 Reduction of the spectrum of forced oscillations

For the construction of an adequate physical model of oscillations, taking into account their forced character, we regard the quartz plate as a simple oscillating system with an external force described by the equation:

$$\ddot{x} + 2\sigma\dot{x} + \omega_0^2 x = \Phi_0 e^{i\omega_0 t}, \quad (5)$$

where the quantity  $\Phi_0$  has the meaning of amplitude of oscillations of the voltage, induced on the electrodes by the quartz plate, attributed to its effective inductance:  $\Phi_0 = V_0/L$ , and the quantity  $x(t)$  is the charge on the coating of the quartz plate. Calculating the Fourier images of the left and of the right hand sides of equation (5), we find:

$$x_\omega = \frac{\Phi_0 \delta(\omega - \omega_0)}{-\omega^2 + 2i\sigma\omega + \omega_0^2}. \quad (6)$$

Actually, the voltage on the plates of the quartz generator is not purely monochromatic and, by virtue of the fact that the quartz generator is the basic element of the auto-generator with feedback circuit, the power spectrum of the given tension is fuzzy in the vicinity of the frequency  $\omega_0$  practically, with the same value  $\sigma$ . Consequently, we have to replace in (6) the delta function by the function:

$$G(1/\sqrt{\pi}\sigma, \sigma, \omega_0, \omega) = \frac{1}{\sqrt{\pi}\sigma} e^{(\omega - \omega_0)^2 / \sigma^2}, \quad (7)$$

taking into account the fuzziness of the oscillations of the voltage, which, by passing to the limit with  $\sigma \rightarrow 0$  is transformed into the delta function  $\delta(\omega - \omega_0)$ . After this modification, the spectrum of forced oscillations takes the form:

$$x_\omega = \frac{\Phi_0}{\sqrt{\pi}\sigma} \frac{e^{-(\omega - \omega_0)^2 / \sigma^2}}{(\omega_0^2 - \omega^2 + 2i\sigma\omega)}, \quad (8)$$

the spectrum of the voltage is

$$V_\omega = L(\omega_0^2 - \omega^2 + 2i\sigma\omega)x_\omega = \frac{V_0}{\sqrt{\pi}\sigma} e^{-(\omega - \omega_0)^2 / \sigma^2}, \quad (9)$$

and the power spectrum of the output voltage is:

$$|U_\omega|^2 = \frac{K^2 V_0^2}{\pi\sigma^2} e^{-2(\omega - \omega_0)^2 / \sigma^2}. \quad (10)$$

Comparing (9) and (3), we are led to the relation between the theoretical start-up parameters of the quartz plate and the observed characteristics of the spectrum (which we will denote by a bar):

$$\omega_0 = \bar{\omega}_0; \quad \sigma = \sqrt{2}\bar{\sigma}; \quad \bar{I} = \frac{K^2 V_0^2}{\pi\sigma^2} = \frac{K^2 V_0^2}{2\pi\bar{\sigma}^2}. \quad (11)$$

formulas (11) are necessary for the comparison of the theoretical calculations with the experimental dependencies and will be used in the following for evaluations.

### 3.1.2 Description of the perturbations

We will describe the exterior effect on the generator with the help of the effective equation of oscillations with friction:

$$\delta\ddot{x} + 2\sigma\delta\dot{x} + \omega_0^2\delta x = \frac{f(t)}{L}, \quad (12)$$

where  $\delta x$  is the size of the perturbation of oscillations,  $f(t)$  is the (limited in time) source of the effect. If, as we mentioned earlier, we interpret the quantity  $x$  as the charge on the quartz plates, then the quantity  $f(t)$  will have the meaning of perturbing voltage on the quartz plates ( $L$  is the inductance of a quartz plate). Passing in (12) to Fourier components, we get:

$$(-\omega^2 + 2i\sigma\omega + \omega_0^2)\delta x_\omega = \frac{f_\omega}{L}, \quad (13)$$

where

$$f_\omega = \frac{1}{2\pi} \int_{-\infty}^{+\infty} f(t)e^{-i\omega t} dt.$$

Therefore, the average power spectrum of the output signal is

$$G' = K^2|V_\omega + f_\omega|^2 \approx G + K^2(V_\omega\delta f_\omega^* + V_\omega^*\delta f_\omega). \quad (14)$$

The difference power spectrum of the output signal will be given by the formula:

$$\Delta G = G' - G = K(U_\omega\delta f_\omega^* + U_\omega^*\delta f_\omega). \quad (15)$$

Taking into account relation (9), we are led after some simple transformations to the final general form of the difference spectrum:

$$\Delta G = 2K\sqrt{I}e^{-(\omega-\omega_0)^2/2\sigma^2} \operatorname{Re} f_\omega. \quad (16)$$

In the following, formula (16) will be used in estimations in concrete models for the effect.

### 3.1.3 Weak deformation of simple resonance curves

Rather than proceeding to concrete estimations, we will explain the general approach for the study of weak deformations of relations of the form:

$$G(I, \omega_0, \sigma, \omega) = Ie^{-(\omega-\omega_0)^2/\sigma^2} = IG(a, \xi). \quad (17)$$

In (17) we also chose for convenience the dimensionless function

$$\mathcal{G}(a, \xi) \equiv e^{-\xi^2/a^2}, \quad \xi = \frac{\omega - \omega_0}{\omega_0}, \quad a = \frac{\sigma}{\omega_0}. \quad (18)$$

The characteristic form of relation (17) is shown in Fig. 13.

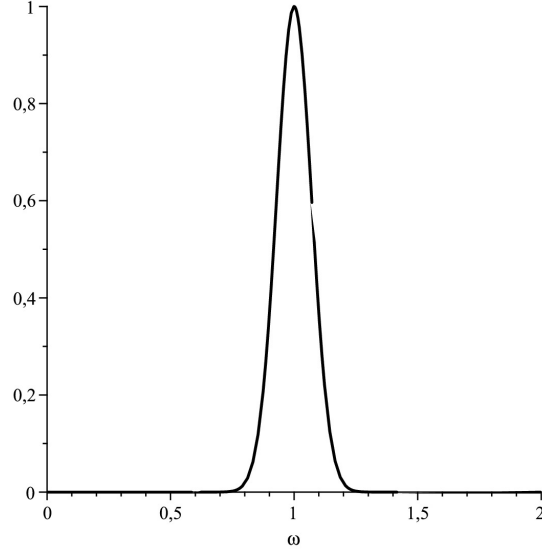


Fig. 13: Characteristic form of the dependence (17),  $I = 1, \sigma = 0.1, \omega_0 = 1$ .

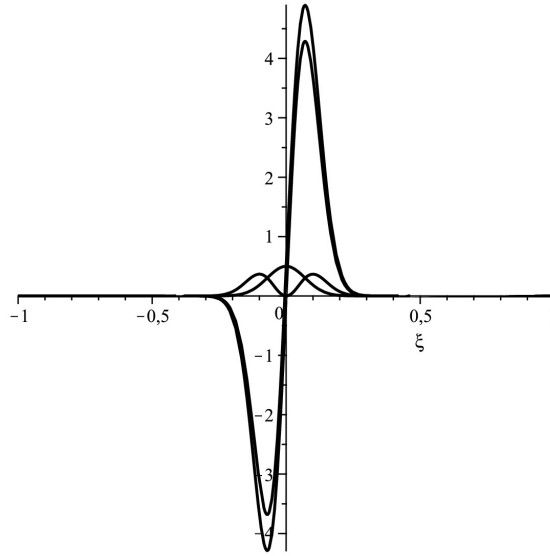


Fig. 14: Possible characteristic forms of the dependence (19). For all the three dependencies  $I = 1, \sigma = 0.1, \omega_0 = 1$ . For symmetric single-hump graph  $\Delta_I = 0.5, \Delta_\omega = \Delta_\sigma = 0$ , for a symmetric two-hump one,  $\Delta_I = \Delta_\omega = 0, \Delta_\sigma = 0.5$ , for an antisymmetric one with oscillation amplitude around 4.3  $\Delta_\omega = 0.5, \Delta_I = \Delta_\sigma = 0$ , and finally, for an antisymmetric  $\Delta_I = \Delta_\sigma = \Delta_\omega = 0.5$ .

Let us assume now that we have a relation of the form (17) with parameters close to each other  $I' = I + \delta I, \omega'_0 = \omega_0 + \delta\omega_0, \sigma' = \sigma + \delta\sigma'$ . Then, the difference  $G(I', \omega'_0, \sigma', \omega) -$

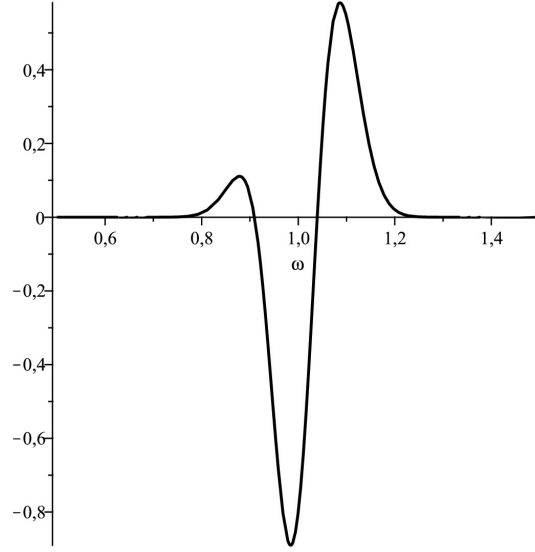


Fig. 15: Relation (19), for values of the parameters taken from (23).

$G(I, \omega_0, \sigma, \omega)$  can be represented in the form:

$$\Delta G(\xi) = IG(a, \xi) \left( \Delta_I + \frac{2\xi}{a^2} (\Delta_\omega + \xi \Delta_\sigma) \right), \quad (19)$$

where

$$\Delta_I = \frac{\delta I}{I}; \quad \Delta_\omega = \frac{\delta \omega_0}{\omega_0}; \quad \Delta_\sigma = \frac{\delta \sigma}{\sigma} \quad (20)$$

are the relative modifications of the parameters of relation (17). The characteristic forms of the difference relation (19) are represented in Fig. 14.

The presented graphs illustrate the fact that the difference spectrum (19) is generally asymmetric (neither symmetric, nor antisymmetric) with respect to the point  $\xi = 0 \quad \omega = \omega_0$ . In the case  $\Delta_\omega = 0$ , the difference curve will be symmetric and in the case  $\Delta_I = \Delta_\sigma = 0$ , antisymmetric. Besides, the perturbations of the parameters are related to the shape of the curve, in particular, to the position of maxima and minima. A simple analysis reveals an inconvenient of the qualitative analysis of the perturbation of the coordinates of maxima and minima, since the calculations with respect to these coordinates lead to cubic equations. Much more simply and more rapidly, the perturbations  $\Delta_I, \Delta_\omega, \Delta_\sigma$  can be calculated by studying the behavior of the function  $\Delta G$  at zero and in its neighborhood. For the interpretation, we take the following formulas, following from (19):

$$\Delta_I = \frac{\Delta G(0)}{I}; \quad \Delta_\omega = \frac{a^2 \Delta G'(0)}{2I}; \quad \Delta_\sigma = \frac{e \Delta G(a) - \Delta G(0) - a \Delta G'(0)}{2I}. \quad (21)$$

Here, the prime sign means differentiation with respect to the dimensionless variable  $\xi$ . These formulas will be used in the following for the interpretation of experimental difference spectra in terms of the variations of the intensity parameters, of the main frequency

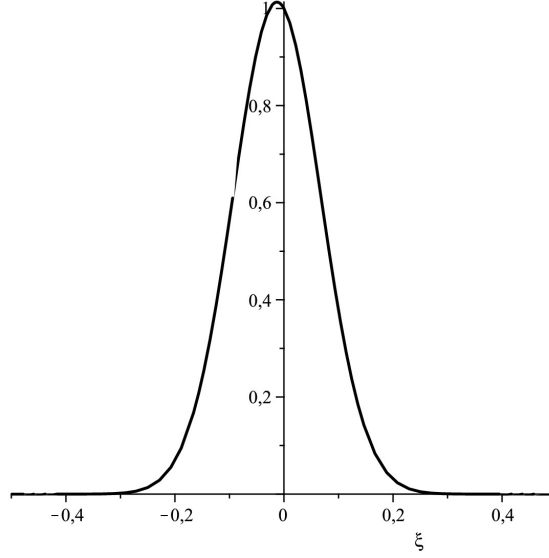


Fig. 16: Dimensionless spectral function (30) for values of the parameters taken from (31).

and of the width of the output spectral curve. As an example, we will interpret in terms of the deformations  $\Delta_I, \Delta_\sigma, \Delta_\omega$  the experimental spectrum presented in Fig. 9. According to the passport data,  $\omega_0 = 10^7 \text{Hz}$ , and according to the Fig. 8 of the power spectrum  $\bar{I} \approx 50 \text{V}^2/\text{Hz}^2$ ,  $\bar{\sigma} \approx 0.8 \cdot 10^6 \text{Hz}$ , it should be  $a \sim 0.08$ . Directly from Fig. 9 of the difference power spectrum, we find:

$$\begin{aligned} \Delta G(0) &\approx -0.08 \text{V}^2/\text{Hz}^2; \\ \Delta G'(0) &\approx 11.5 \text{V}^2/\text{Hz}^2; \\ \Delta G(a) &\approx G(0) + aG'(0) \approx 0.84 \text{V}^2/\text{Hz}^2. \end{aligned} \quad (22)$$

Replacing these data in the interpretation formulas (21), we get:

$$\begin{aligned} \Delta_I &\approx -1.6 \cdot 10^{-3}; \\ \Delta_\omega &\approx 7.4 \cdot 10^{-4} \\ \Delta_\sigma &\approx 1.4 \cdot 10^{-2}. \end{aligned} \quad (23)$$

In Fig. 15, it is represented the theoretical difference relation (19) with the parameters (23).

### 3.2 Estimation of the influence of acoustic oscillations

Acoustic waves generated by the strike of the weight on the anvil will be considered as the main factor able to influence on the work of the quartz generator. We will examine a model in which the acoustic impulse generated by the strike is described by a signal of the form:

$$X(t) = X_0 e^{-\Sigma t} e^{i\Omega t} \quad (24)$$

where  $\Omega$  is the main frequency of acoustic oscillations,  $\Sigma$  is the parameter of their decreasing, and by the corresponding spectrum:

$$X_\omega = \frac{iX_0}{2\pi(\Omega - \omega + i\Sigma)}, \quad (25)$$

The quantity  $X_0$  has the meaning of amplitude of the oscillations of the surface in the neighborhood of the strike. Oscillations of the floor with the amplitude  $X_0$  and frequency  $\Omega$  induce a variable field of inertia, having the amplitude of the order of  $\Omega^2 X_0$ . This field creates a field of tensions inside the quartz plates, oscillating (in time) with the amplitude  $\delta\mathcal{T} \sim \mu\Omega^2 X_0/S \sim k\rho\ell\Omega^2 X_0$ , where  $\mu = k\rho\ell S$  is the attached mass of the plate (it is less than the real mass because of the damping devices which reduce the effect of jolting,  $k$  is the coefficient of damping,  $\ell$  is the thickness of the plate and  $S$ , the area of its transversal section. These stresses create additional variable fields of deformation (with respect to the nominal ones), with the amplitude  $\delta u \sim \delta\mathcal{T}/E \sim k\rho\ell\Omega^2 X_0/E$ , where  $E$  is the Young modulus of quartz. The additional deformations induce an additional perturbing stress on the quartz plates, whose amplitude can be estimated by means of the formula:

$$\delta V_0 \sim \frac{\delta u}{d}\ell \sim \frac{k\rho\ell^2\Omega^2 X_0}{Ed} \sim \frac{k\ell^2\Omega^2 X_0}{dc_q^2}, \quad (26)$$

where  $d$  is the piezo-modulus of quartz,  $c_q^2 = E/\rho$  is the squared speed of sound in quartz. Thus, combining (25) and (26), we are led to the formula:

$$f_\omega = \frac{ik\ell^2\Omega^2 X_0}{2\pi dc_q^2(\Omega - \omega + i\Sigma)} = \frac{i\delta V_0}{2\pi(\Omega - \omega + i\Sigma)}. \quad (27)$$

Computing the real part of the quantity  $f_\omega$ , we find:

$$\text{Re } f_\omega = \frac{\delta V_0}{2\pi\omega_0} \frac{\alpha}{(\xi + \xi_0)^2 + \alpha^2}, \quad (28)$$

where  $\xi_0 = (\omega_0 - \Omega)/\omega_0$ ,  $\alpha = \Sigma/\omega_0$ . Substituting this expression into the general formula (16), we obtain for the acoustic difference spectrum the following relation:

$$\Delta G_{\text{ac}}(\xi) = \frac{\alpha K \delta V_0 \sqrt{I}}{\pi\omega_0} \mathcal{G}_{\text{ac}}(a, \alpha, \xi_0, \xi), \quad (29)$$

where we have introduced the dimensionless difference spectral function of the acoustic perturbation:

$$\mathcal{G}_{\text{ac}}(\bar{a}, \alpha, \xi_0, \xi) \equiv \frac{e^{-\xi^2/2\bar{a}^2}}{(\xi + \xi_0)^2 + \alpha^2}, \quad (30)$$

and  $\bar{a} = \bar{\sigma}/\omega_0$ .

Now, we can pass to concrete quantitative evaluations. By qualitatively analyzing the records of the acoustic signal, we notice that we can distinguish in it more or less clearly a low-frequency component of the order of kilo-Hertz and its ultrasound filling with several

times smaller amplitudes. Besides, the duration of the acoustic impulse is if the order of 10 milisec. Therefore, we get the working estimates for the acoustic frequency parameters of relation (29):

$$\xi_0 \approx 1, \quad \alpha \approx 10^{-5}. \quad (31)$$

Now, we can build an approximate graph of the dimensionless spectral function (30) — it is represented in Fig. 16.

This graph is qualitatively different from the experimental one and testifies about the dominance of the amplitude shift with respect to the shifts of the other parameters.

For the estimation of the amplitude spectrum, we obtain the following reference [19], on the estimative data for the parameters entering  $\delta V_0$ :

$$k \sim 0.1; \ell \sim 10^{-3} \text{m}; \Omega \sim 10^3 \text{Hz}; X_0 \sim 10^{-3} \text{m}; d \sim 10^{-10} \frac{\text{C}}{\text{N}}. \quad (32)$$

Starting from these estimates, we get for the coefficient of the dimensionless spectral function in (29), a quantity of the order  $10^{-10} \text{V}^2/\text{Hz}^2$ .

Calculating now by (29) the values  $\Delta G_{\text{ac}}(0)$ ,  $\Delta G'_{\text{ac}}(0)$  and  $\Delta G_{\text{ac}}(a)$ :

$$\begin{aligned} \Delta G_{\text{ac}}(0) &\approx 10^{-10} \text{V}^2/\text{Hz}^2, \\ \Delta G'_{\text{ac}}(0) &\approx -2 \cdot 10^{-10} \text{V}^2/\text{Hz}^2, \\ \Delta G_{\text{ac}}(a) &\approx 5 \cdot 10^{-11} \text{V}^2/\text{Hz}^2, \end{aligned} \quad (33)$$

and, substituting the obtained values in formulas (21), we find for the acoustic relative shifts the following values:

$$\Delta_I^{\text{ac}} \sim 2 \cdot 10^{-12}; \quad \Delta_\omega^{\text{ac}} \sim -1.3 \cdot 10^{-14}; \quad \Delta_\sigma^{\text{ac}} \sim 6 \cdot 10^{-13}. \quad (34)$$

These estimates differ approximately by 10 orders from the experimental data (23). We are led to the conclusion that neither the form of the difference spectrum of acoustic perturbations, nor (even less) the order of magnitude of the amplitude of the perturbation do not correspond to the ones observed in the experiment.

### 3.3 Estimation of the electromagnetic influence of the strike

We will deduce in the following some estimating formulas for the electromagnetic influence of the strike of the weight on the functioning of the quartz generator. Despite the shielding of the equipment, the electromagnetic impulse has the ability to permeate it and, as we will see in the following, it can influence, in principle, the functioning of the quartz generator, by changing its spectral function.

In the beginning, we will describe the essence of the processes which take place in a qualitative manner. During the strike of the steel weight on the anvil, in the places of contact of the weight with the anvil, there appear stresses which are significant by size and strongly non-stationary, producing a strong deformation of the crystal lattice and the shift of its electron and ion components with respect to each other. The appearance and disappearance of such a polarized state is accompanied by a radiation of the electromagnetic impulse. Its non-coherent character leads to the equality  $\langle \vec{E} \rangle = 0$ , though,

this impulse brings in any element of the spatial angle momentum and energy. A part of this momentum and energy passes through the screens and reaches the quartz plate. The interaction of the electromagnetic impulse and the oscillating plate is reduced to a short-term mechanical "shake" of the quartz crystal by the radiation pressure of the impulse, which produces the deformation of the spectral function. We will pass to a model estimation. First of all, we will estimate the integral intensity of the electromagnetic impulse generated by the strike of the weight on the base. According to the general theory of electromagnetic radiation [20], the order of magnitude of the (main) dipole component of the radiation is given by the expression:

$$J \sim \frac{\ddot{P}^2}{\varepsilon_0 c^3}. \quad (35)$$

In (35), the quantity  $P$  represents the mechanically induced dipole moment in the process of hitting. In order to estimate the quantity  $P$ , we will admit that during the strike, the electronic (more mobile) component of the electron-ion crystal lattice acquires the speed  $v$ , with which the weight moves on the anvil immediately before the strike. Then, the energy conservation law yields:

$$m_e n_e V v^2 \sim \frac{Q^2}{C}, \quad (36)$$

where  $Q \sim en_e S l$  is the polarization charge induced by the strike,  $n_e$ , the concentration of electrons,  $S$ , the area of the section of the weight,  $l$  — the size of the shift of the electron and ion components with respect to each other,  $C \sim \varepsilon_0 \varepsilon(\omega) S/d$  — the capacitance of the weight,  $d$  — its thickness (its size in the perpendicular direction to the plane of contact). From (36), by means of the relation  $v^2 \sim gh$ , ( $h$  is the height from which the weight falls) we get:

$$P \sim Q l \sim \frac{\varepsilon_0 \varepsilon m_e g h S}{e}. \quad (37)$$

The process of separation of the component of metallic plasma during the strike leads to Langmuir oscillations, during which a part of the polarization energy is transformed (decays) into radiation. The frequency of the Langmuir oscillations is  $\omega_L \sim \sqrt{n_e e^2 / \varepsilon_0 m_e}$ , each differentiation with respect to time in (35) reduces to a multiplication by  $\omega_L$ , thus, we finally get for the intensity of the dipole radiation the estimate:

$$J \sim \frac{(\varepsilon_L n_e)^2 (g h S)^2}{\varepsilon_0 c^3}. \quad (38)$$

The energy  $I \Delta t$  radiated in the striking process, on a duration of  $\Delta t$ , is spread outside in the form of a spherical layer with thickness  $c \Delta t$ . For the estimation of the energy density  $\epsilon$ , in the radiation impulse, in the place where the generator is located, we set

$$J \Delta t \sim \epsilon \cdot 4\pi r^2 c \Delta t, \quad (39)$$

therefore

$$\epsilon \sim 10^{-1} \frac{J}{r^2 c}, \quad (40)$$

where  $r$  is the distance from the place of the strike to the generator. This way, the impulse of the radiation which reaches the quartz plate creates in it an acceleration impulse:

$$\varphi \sim \frac{F}{M} \sim \frac{p\Delta S}{M} \sim \frac{q\epsilon\Delta S}{M}, \quad (41)$$

where  $M$  is the mass of the quartz plate,  $\Delta S$  is its area,  $q$  is the integral coefficient of absorption of the electromagnetic energy-momentum during its spreading from the place of the strike to the generator. Finally, after substituting in (41) (38) and (40), we get:

$$\varphi \sim 10^{-1} \frac{q}{\epsilon_0 c^4 r^2} \cdot \frac{\Delta S}{M} \cdot (\epsilon_L \epsilon n_e)^2 (ghS)^2. \quad (42)$$

Repeating now "word for word" the estimative calculations in the previous paragraph, which relate the acceleration field to the amplitude of the perturbing stress, we get, by virtue of formula (26):

$$\delta V_0 \sim \frac{k\ell^2}{dc_q^2} \varphi \sim 10^{-1} \frac{q}{\epsilon_0 c^4 r^2} \cdot \frac{k\ell}{\rho_q c_q^2 d} \cdot (\epsilon_L \epsilon n_e)^2 (ghS)^2. \quad (43)$$

In the estimate (43), the first factor is related to the process of radiation and spreading of the electromagnetic radiation, the second one, to the structure of the quartz plate, the third, to the electronic structure of the weight and the fourth one, to the mechanical parameters of the experiment itself.

Let us suppose now that the electromagnetic perturbation which acts on the quartz plate has, in a rough approximation, a rectangular dependence on time, i.e., it is described by a function of the form:

$$f(t) = \delta V(t) = \begin{cases} 0, & t < 0; \\ \delta V_0, & 0 \leq t \leq \tau; \\ 0, & t > \tau, \end{cases} \quad (44)$$

where  $\tau$  is the time of the (simple, unique) impact. The Fourier transform of relation (44) has the form:

$$f_\omega = \frac{i\delta V_0}{2\pi\omega} (e^{-i\omega\tau} - 1). \quad (45)$$

Its real part is:

$$\text{Re } f_\omega = \frac{\delta V_0}{2\pi\omega} \sin(\omega\tau). \quad (46)$$

Substituting this expression into the general formula (16), we get:

$$\Delta G_{\text{em}}(\xi) \approx \frac{K\sqrt{I}\delta V_0}{\pi\omega_0} \mathcal{G}_{\text{em}}(\bar{a}, \beta, \xi), \quad (47)$$

where we have introduced the dimensionless electromagnetic function of difference power spectrum

$$\mathcal{G}_{\text{em}}(\bar{a}, \beta, \xi) = e^{-\xi^2/2\bar{a}^2} \frac{\sin(\beta(\xi+1))}{\xi+1}, \quad (48)$$

and  $\beta = \omega_0\tau$ .

Let us pass to concrete quantitative estimations. The experimental data give for the time of the strike, the quantity  $\sim 1/\Sigma \sim 10\text{ms}$ , which represents the characteristic time of attenuation of the acoustic impulse and includes effects of rattle during its complex (asymmetric) strike on the anvil. On the contrary, the time  $\tau$ , which defines the electromagnetic impulse, is a time of a unique simple impact, whose size, according to evaluations of the contact problem in elasticity theory [21] represents a quantity <sup>4</sup> of the order  $10^{-1}\text{ms}$ , which does not contradict the experimental data we have. Thus, for the quantity  $\beta$ , we get the estimation:  $\beta \sim 10^3$ .

Now, we can build an approximate graph of the dimensionless spectral function (48) — it is represented in Fig. 17.

The above graph is essentially different from the experimental one — one cannot generally interpret it in terms of the difference of two close peaks! Moreover, if we take into account the fact that the experimental spectrum was obtained by averaging over various strikes, in which it was observed the time dispersion, then the effect must, in general, practically vanish, having in mind the randomness of the phases which are added, corresponding to separate strikes. Let us suppose, for the evaluation, that the times of the strikes are equally distributed in the interval  $[\tau_0 - \Delta\tau/2; \tau_0 + \Delta\tau/2]$ , with  $\Delta\tau = \tau_0/10$ . Then, the averaging of the spectrum (47) by  $\tau$  reduces to integration on the interval  $[\tau_0 - \Delta\tau/2; \tau_0 + \Delta\tau/2]$  of the function  $\sin(\beta(\xi+1))$  and division of the result to  $\Delta\tau$ . If we perform such an averaging, then, for the time averaged difference spectrum of electromagnetic perturbations, we get the following formula:

$$\langle \mathcal{G}_{\text{em}} \rangle = \mathcal{G}_{\text{em}} \cdot \frac{\sin(\Delta\beta(\xi+1)/2)}{\Delta\beta(\xi+1)/2}, \quad (49)$$

where  $\Delta\beta = \Delta\tau\omega_0 \sim 10^2$ . The graph of the function (49) is presented in Fig. 18.

The comparison of the amplitudes of the graphs to the right in Fig. 17 and Fig. 18 clearly illustrates the role of the averaging — the amplitude of the difference spectrum after the averaging decreased about 50 times.

Still, we will estimate this amplitude, based on the reference [19] and on the estimative data for the parameters entering  $\delta V_0$  in (32) and on the following:

$$\begin{aligned} r &\sim 1\text{m}, \\ \rho_q &\sim 10^3\text{kg/m}^3, \\ n_e &\sim 10^{28}\text{m}^{-3}, \\ S &\sim 10^{-1}\text{m}^2, \\ \Delta S &\sim 10^{-4}\text{m}^{-2}, \\ gh &\sim 10\text{m}^2\text{s}^2, \\ \varepsilon_L &\sim 1, \quad q \sim 10^{-4}. \end{aligned} \quad (50)$$

<sup>4</sup>The estimate (problem 1 in paragraph 9 in [21]) has, in our case, the form:

$$\tau \sim \left( \frac{m^2}{(gh)^{1/2}RE^2} \right)^{1/5},$$

where  $m$  is the mass of the weight,  $h$ , the height of its fall,  $E$ , the Young modulus of steel,  $R$ , the radius of the weight.

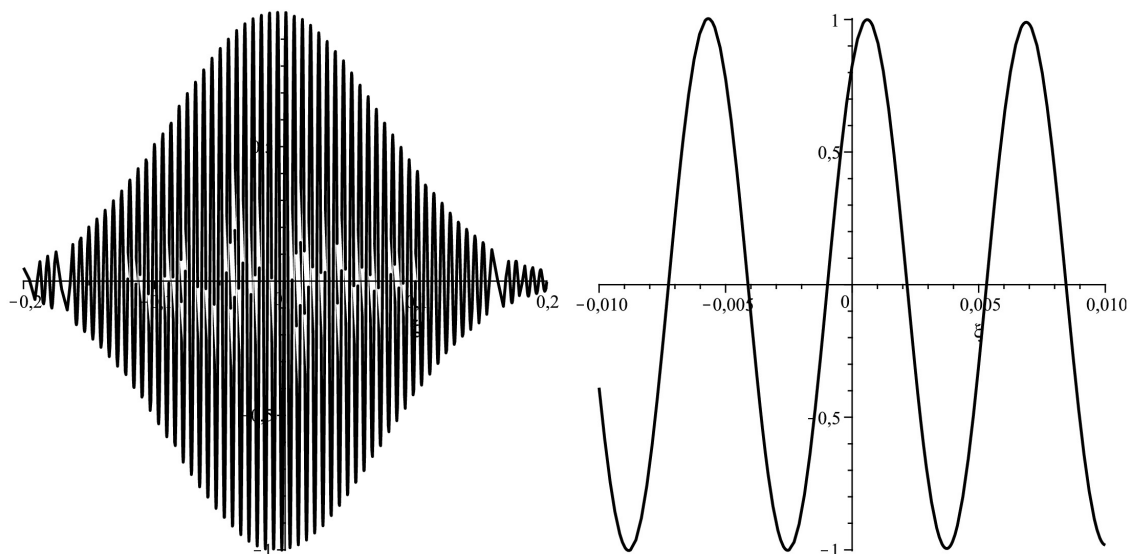


Fig. 17: Dimensionless spectral function (48) for the parameter values  $\bar{a}=0.08$ ,  $\beta \sim 10^3$  (to the right, a magnified fragment in the neighborhood of  $\xi = 0$ .)

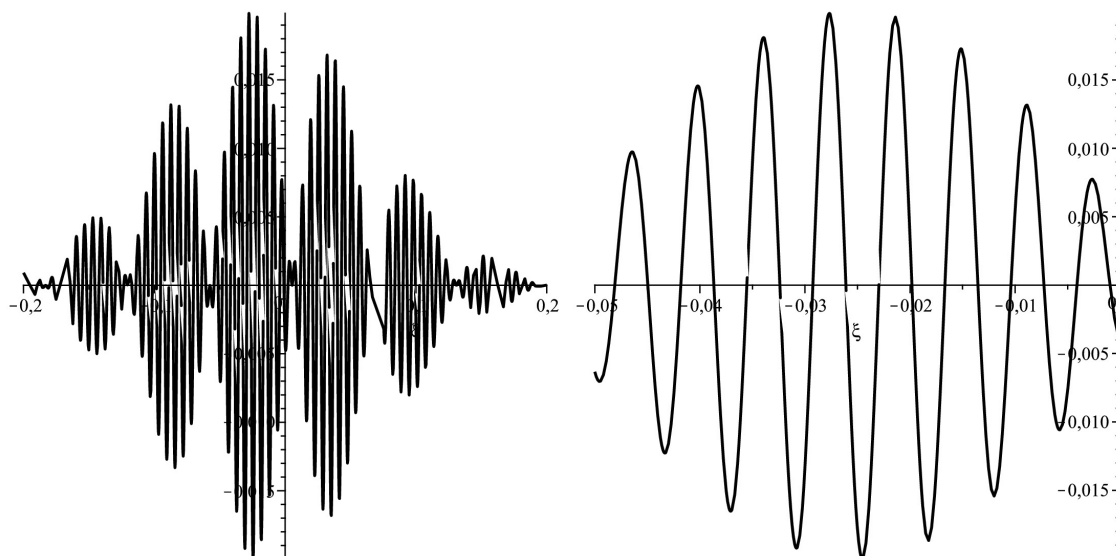


Fig. 18: Averaged dimensionless spectral function (49) for the parameter values  $\bar{a} = 0.08$ ,  $\beta \sim 10^3$ ,  $\Delta\beta \sim 10^2$  (to the right, a magnified fragment in the neighborhood of the maximum).

Starting with these estimations, we get for the amplitude of the difference spectrum function in (47), a value which does not exceed  $10^{-18} \div 10^{-20} \text{ V}^2/\text{Hz}^2$ . This estimation differs from the amplitudes of the experimental power spectrum with about 20 orders of magnitude. This way, *the shape of the difference spectrum of the electromagnetic perturbations and the order of magnitude of its amplitude do absolutely not correspond to the experimentally observed picture.*

### 3.4 Estimation of the wave-gravitational perturbation

In this section, we will roughly evaluate the order of magnitude of the contribution of the gravitational radiation to the shift of the frequency of the quartz generator. As a basis, we will take the theory of radiation of weak gravitational waves in general relativity theory [20]. In this theory, for the wave perturbation of the metric background, it is obtained the following estimation:

$$h \sim \frac{\kappa}{r} \ddot{D}, \quad (51)$$

where  $\kappa$  is Einstein's gravitational constant, equal to  $8\pi G/c^4$ ,  $r$  is the distance from the system which radiates the waves to the observation point,  $\ddot{D}$ , the characteristic value of the second derivative of the quadrupole moment of the gravitationally radiating system. Since the main part of the gravitational radiation is generated during the strike and the strike of the weight on the anvil can be roughly regarded as an oscillation process with period  $\tau$  and amplitude  $\delta$  (deformation amplitude) at the place of contact, the quantity  $\ddot{D}$  can be estimated as  $M\delta^2/\tau^2$ , where  $M$  is the mass of the weight. Thus, for the amplitude of the perturbation of the metric, we get the following expression:

$$h \sim \frac{\kappa}{r} M \frac{\delta^2}{\tau^2}. \quad (52)$$

The perturbations of the metric modify, in their turn, lengths and time intervals, besides, taking into account the smallness of the perturbation and the simple relation between frequency and time gauges, the order of magnitude  $h$  of the perturbation coincides with the order  $\Delta_{\text{grav}}$ . Substituting the numerical values, we get the following estimation:

$$\Delta_{\text{grav}} \sim 10^{-44}, \quad (53)$$

which is by many orders less than the observed quantity  $\Delta$ . We can definitely conclude that *gravitational radiation is not related to the observed effect.*

## 4 Conclusion

We have developed a method of interpretation of difference output power spectra of a quartz generator (Section 3.1.3) in terms of the deformation of the parameters of the Gaussian peak, a method of simplified, but self-consistent description of the functioning of the auto-oscillation scheme (Section 3.1.1) and a method of calculation of its perturbations (formula (16)). Based upon these, we have provided an interpretation of one of

the characteristic spectra (Fig. 9), obtained in the experiment. We present in brief the obtained results.

1. The sizes of the relative deformations of the parameters of the Gaussian power spectra obtained from experimental data, interpreted by means of the above developed method, have the following (approximate) values:

$$\Delta_I \approx -1.6 \cdot 10^{-3}; \quad \Delta_\omega \approx 7.4 \cdot 10^{-4}; \quad \Delta_\sigma \approx 1.4 \cdot 10^{-2}. \quad (54)$$

Their inaccuracy is defined by the inaccuracy of the calculation of the spectrum in the computer and (mainly) by the inaccuracy of the reference values of the difference spectrum according to the graph and, all in all, has the order of 10 – 20%.

2. The difference power spectrum of the acoustic perturbations has a dominating order of magnitude (with respect to amplitude), among spectra of other factors (gravitational and electromagnetic), but its shape (Fig. 16) differs from the experimental one (the contribution of the deformation of the frequency is strongly underestimated), and the order of magnitude of the amplitude differs approximately by 10 orders from the experimental values.
3. The difference power spectrum of the electromagnetic perturbation has to be examined as the second in size (with respect to amplitude), among spectra corresponding to other factors, but its shape (Fig. 17) is essentially different from the experimental one (generally, one cannot interpret it as a deformation of the parameters of the Gaussian peak). The order of magnitude of the amplitude differs by approximately 20 orders from the experimental values. Besides, the difference will only increase if we take into account the averaging of spectra corresponding to strike times.
4. The wave-gravitational relativistic effect of frequency shift, related to the deformation of space-time scales, differs by around 40 orders from the experimental data of shifts of the parameters.

Thus, based on the obtained estimates, we can state with confidence that *none of the examined mechanisms — acoustic, electromagnetic or wave-gravitational — is able to completely explain the nature of the deformation of the power spectrum of the signal of the quartz generator — either from a qualitative or from a quantitative point of view. This brings a proof to the cautious assumption of the possibility of generating hyperbolic fields in the process of a mechanical strike.*

The above conclusion certainly needs a more careful check both in what concerns the experiment method and its theoretical interpretation. The refinement of the estimative values of the parameters most likely cannot correct theoretical predictions by 10 degrees. At present, *the obtained results can be regarded as preliminary ones, an encouraging evidence of the presence of new physical effects, which cannot explained in the framework of existent physical theories.*

## References

- [1] Bogoslovsky G.Yu. and Goenner H.F., Phys. Let. A **244**, no. 4, (1998), p. 222.
- [2] Bogoslovsky G.Yu. and Goenner H.F., Gen. Relativ. Gravit., **31**, no. 10, (1999), p. 1565.
- [3] Pavlov D.G., *Hypercomplex Numbers, Associated Metric Spaces and Extension of Relativistic Hyperboloid*, ArXiv:gr-qc/0206004.
- [4] Pavlov D.G., *4-dimensional time as an alternative to Minkowski space-time*, Proceedings of the International Conference «GEON-2003», Kazan, 2003.
- [5] Pavlov D.G., *Generalization of the scalar product axioms*, Hypercomplex Numbers in Geometry and Physics, **1**(1) (2004), 5-19.
- [6] Pavlov D.G., *Chronometry of three-dimensional time*, Hypercomplex Numbers in Geometry and Physics **1**(1) (2004), 20-32.
- [7] Pavlov D.G., *Four-dimensional time*, Hypercomplex Numbers in Geometry and Physics, **1**(1) (2004), 33-42.
- [8] Garas'ko G.I., *Generalized-analytic functions of a polynumber variable*, Hypercomplex Numbers in Geometry and Physics **1**(1) (2004), 75-88.
- [9] Lebedev S.V., *Properties of spaces associated to the commutative-associative algebras  $H_3$  and  $H_4$* , Hypercomplex Numbers in Geometry and Physics **1**(1) (2004), 68-74.
- [10] Siparov S.V., *Canonical Hamilton equations and the Berwald-Moor metric*, Hypercomplex Numbers in Geometry and Physics, **2**(4) (2005) 51-56.
- [11] Zaripov R.G., *The relation of simultaneity in a Finslerian space-time*, Hypercomplex Numbers in Geometry and Physics **1**(5) (2006), 27-46.
- [12] Garas'ko G.I., *Foundations of Finsler geometry for physicists*, Moscow, Tetru, 2009.
- [13] Pavlov D.G. and Kokarev, S.S., *Conformal gauges of Berwald-Moor geometry and nonlinear symmetries induced by these* Hypercomplex Numbers in Geometry and Physics **2**(10) (2008) 3-14.
- [14] Pavlov D.G., *A hyperbolic analogue of the electromagnetic field*, Hypercomplex Numbers in Geometry and Physics **1**(13) (2010), 3-15.
- [15] Pavlov D.G. and Kokarev, S.S., *Hyperbolic field theory in the plane of a double variable*, Hypercomplex Numbers in Geometry and Physics **1**(13) (2010), 78-127.
- [16] Pavlov D.G. and Kokarev, S.S., *Analytic, differential-geometric and algebraic properties of smooth functions of a polynumber variable*, Hypercomplex Numbers in Geometry and Physics **16**, (2011).

- [17] Pavlov D.G. and Kokarev, S.S., *h-holomorphic functions of a double variable and their applications*, Hypercomplex Numbers in Geometry and Physics **13** (2010), 44-77.
- [18] Pavlov D.G. and Kokarev, S.S., *Algebraic unified theory of space-time and matter on the plane of a double variable*, Hypercomplex Numbers in Geometry and Physics **2**(14), no. 7, (2010), 11-37.
- [19] Grigoriev, I.S. and Meizlikhov, E.Z., (editors) *Physical Quantities (handbook)*, Moscow, Energoizdat, 1991.
- [20] Landau L.D. and Lifshitz E.M. *Field Theory*, Moscow, Nauka, 1973.
- [21] Landau L.D. and Lifshitz E.M. *Elasticity Theory*, Moscow, Nauka, 1987.